JOURNAL OF SOLID STATE CHEMISTRY **129,** 117–122 (1997)
ARTICLE NO. SC967245

Manifestation of the Cooperative Jahn–Teller Effect in the Raman Spectra of $Ba_2Cu_xZn_{1-x}WO_6$ Mixed Crystals

B. L. Ramakrishna

Arizona State University, Center for Solid State Science, P.O. Box 871704 Tempe, Arizona 85287-1704

D. Reinen

Fachbereich Chemie and Zentrum fuer Materialwissenschaften, Philipps-Universität, Hans-Meerweinstrasse 1, D-35043 Marburg, Germany

and

M. Atanasov[1]

Institute of General and Inorganic Chemistry, Bulgarian Academy of Sciences, 1113 Sofia, Bulgaria

Received July 15, 1996; in revised form November 20, 1996; accepted November 27, 1996

Raman spectra of $Ba_2Cu_xZn_{1-x}WO_6$ mixed crystals ($x = 0.0$ to 0.4 and $x = 1$) are reported and shown to display considerable enhancement of Raman intensity for the WO_6 vibration with $E_g(O_h)$ symmetry when increasing the concentration of Cu^{2+}. Ab initio calculations of Raman frequencies and intensities for a $W(OH)_6$ model cluster indicate that the $A_{1g}(D_{4h})$ component of this vibration may gain considerable intensity via mixing with the totally symmetric stretching A_{1g} (O_h) vibration when lowering the symmetry from O_h to D_{4h}, thus reflecting an indirect influence of Jahn–Teller distorted CuO_6 centers on neighboring WO_6 octahedra. Similarly striking is the change of the Raman spectrum in the energy region of the T_{2g} modes, when switching from the cubic phase with disordered local distortions in the CuO_6–WO_6 frame to the long-range cooperative Jahn–Teller order in Ba_2CuWO_6. It is concluded that Raman spectra can be used as a rather sensitive probe for detecting Jahn–Teller distortions in mixed crystals, thus providing a valuable addition to other spectroscopic techniques.

I. INTRODUCTION

There has been convincing manifestations of the Jahn–Teller effect in stereochemistry and near IR, optical, and EPR spectroscopies of hexacoordinate Cu^{2+} (1, 2). The ^2E_g electronic ground state of octahedral CuO_6 is electronically unstable and couples to vibrations of E_g symmetry, yielding absolute minima in the potential energy surface of the ground state with the typical pattern of tetragonal elongations along the three fourfold axes. In solids, elastic (lattice-mediated) interactions between distorted octahedra may lead to sterical correlations of the local distortions, which reduce the symmetry of the unit cell by lower symmetry cooperative strains and eventually lower one minimum with respect to the other two. At a given concentration of Cu^{2+} ions the strains which are random in a cubic phase may become oriented giving rise to a spontaneous lattice deformation (structural phase transition). An illustrative example for the cooperative Jahn–Teller effect are double perowskite (elpasolite) $Ba_2Cu_xZn_{1-x}WO_6$ mixed crystals ($x = 0.0$–1.0) (1, 3). In Ba_2CuWO_6 tetragonally elongated CuO_6 octahedra [Cu–O bond distances: 1.98 Å (4×), 2.42 Å (2×)] alternate with slightly tetragonally compressed WO_6 octahedra [W–O bond distances 1.96 Å (4×) and 1.90 Å (2×)], (Fig. 1), in contrast to cubic Ba_2ZnWO_6 with regular octahedra of M^{II}–O and W^{VI}–O (bond distances of 2.13 and 1.93 Å, respectively). When the Cu^{2+} concentration reaches a critical value, 0.2, at 300 K, a structural phase transition takes place (Fig. 2a), lowering the symmetry from cubic ($Fm3m$) to tetragonal ($I4/mmm$). It is accompanied by a discontinuous enhancement of the ^2E_g ground state splitting which further increases monotonically with increasing Cu^{2+} content above the critical concentration—as evidenced from the d–d transitions between $^2B_{1g}$ (dx^2–y^2 ground state) and $^2A_{1g}$ (dz^2-excited state) observed in the near IR (see Fig. 2b). A phase diagram is shown in Fig. 2c. In this paper we present Raman spectra of mixed crystals $Ba_2Zn_{1-x}Cu_xWO_6$ ($x = 0.0$–1.0) which

[1]To whom all correspondence should be addressed at Fachbereich Chemie der Philipps-Universität, Hans-Meerweinstrasse 1, D-35043 Marburg, Germany.

0022-4596/97 $25.00

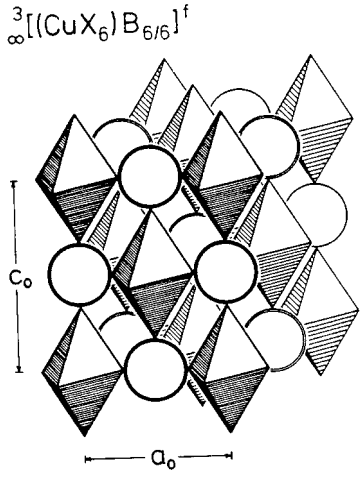

FIG. 1. The crystal structure of Ba_2CuWO_6 with tetragonally elongated CuO_6 octahedra (ferrodistortive order). The W^{IV} ions are indicated by open circles (adopted from Ref. 1).

display interesting changes in dependence on x. Spectra, supplemented by ab-initio calculations of vibrational frequencies and Raman intensities are shown to provide a valuable tool for detecting the geometric changes around non-Jahn–Teller centers (WO_6). Raman spectra of Ba_2CuWO_6 are reported and shown to be particularly informative with respect to the Jahn–Teller active CuO_6 clusters.

II. EXPERIMENTAL SECTION

Sample preparations have been described previously (3). Raman spectra were recorded at 300 K, the technique being described elsewhere (4). They are interpreted on the basis of a factor group analysis within the *Fm3m* space group for the Ba_2ZnWO_6 and the *I4/mmm* space group for the Ba_2CuWO_6 solid. Raman frequencies, their relative intensities, and the changes with x, are rationalized by ab initio calculations, using effective core potentials of regular and tetragonally compressed octahedral $W(OH)_6$ model clusters and the ab initio program GAMESS (General Atomic and Molecular Electronic Structure System), developed by Schmidt *et al.* (5) and adopting the Stevens, Basch, and Krauss (SBK) basis sets (6). The calculations do not include adjustable (fitting) parameters. In order to study the influence of cooperative strains on the Raman vibrations we consider distortions of the WO_6^{6-} polyhedra and introduce one proton for each O^{2-} with a linear W–O–H geometry in order to counterbalance the excess negative charge. In a first step a geometry optimization (O_h symmetry) of the W–O and O–H bond distances has been done yielding bond distances of 1.868 and 0.951 Å, respectively. In a second step harmonic force constants (K_i) and polarizability tensor components α_{kl} ($k, l = x, y, z$) have been calculated in dependence on displacements due to the normal modes Q_i, ($i = 1$ to 5, Fig. 3)

$$\alpha_{kl} = \alpha^0_{kl} + (d\alpha_{kl}/dQ_i)_0\, Q_i. \qquad [1]$$

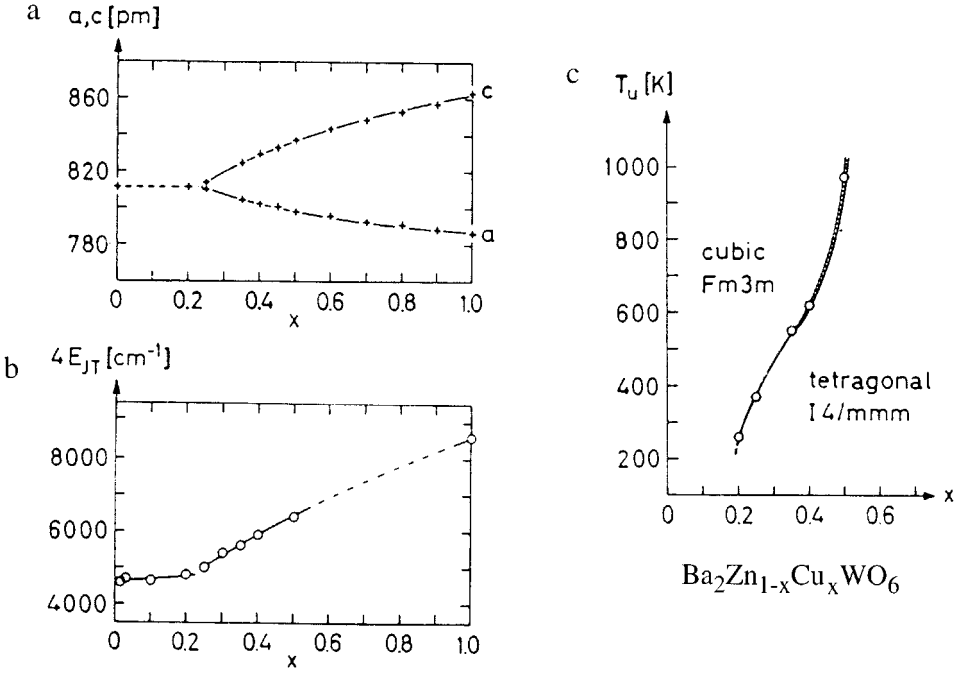

FIG. 2. The unit cell parameters (a), the ^2E_g ground state splitting (b), and the transition temperatures from cubic to tetragonal (c) of mixed crystals $Ba_2Zn_{1-x}Cu_xWO_6$ dependent on the Cu^{2+} concentration (adopted from Ref. 1).

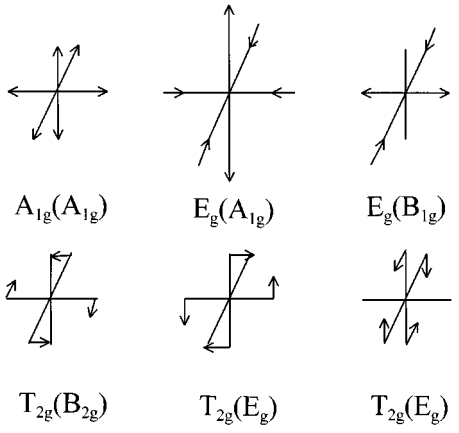

FIG. 3. The Raman active modes of octahedral MO_6 polyhedra and their D_{4h} symmetry labels (in parentheses).

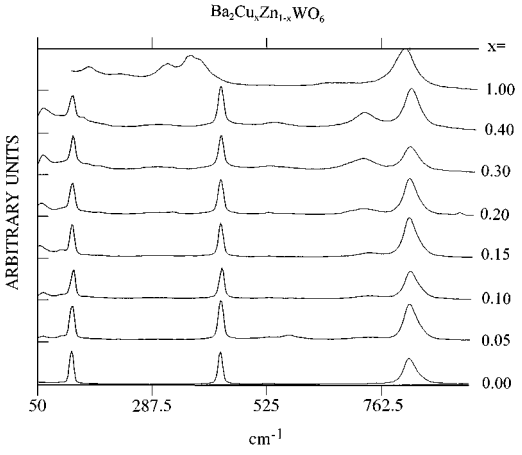

FIG. 4. The Raman spectra of $Ba_2Zn_{1-x}Cu_xWO_6$ mixed crystals (at 300 K).

The intensities of the Raman transitions are approximated by

$$I(Q_i) \propto (d\alpha_{kl}/dQ_i)_0^2. \qquad [2]$$

The same procedure has been followed when considering tetragonally compressed $W(OH)_6$ polyhedra. In tetragonal symmetry the θ component of the octahedral E_g mode is totally symmetric and mixes with the $A_{1g}(A_{1g})$ stretching vibration. The off-diagonal force field parameter K_{12}

$$K_{12} = (d^2V/dQ_{A1}Q_\theta)_0 \qquad [3]$$

defines the matrix which yields the mixing coefficients c_1 and c_2 of the normal modes $A_{1g}(1)$ and $A_{1g}(2)$

$$\begin{matrix} A_{1g}(A_{1g}) & A_{1g}(E_g) \end{matrix}$$
$$\begin{pmatrix} K_{11}-K & K_{12} \\ K_{21} & K_{22}-K \end{pmatrix}\begin{pmatrix} c_1 \\ c_2 \end{pmatrix} = \begin{pmatrix} 0 \\ 0 \end{pmatrix}. \qquad [4]$$

and the diagonalized force field parameters K: K_1 and K_2 in D_{4h}. The K_{ij} force constants are calculated using total energies taken from ab initio calculations. Finally, the polarizability tensor components of the D_{4h}-distorted octahedra are calculated using the same procedure as in O_h, allowing one to deduce the influence of geometrical distortions on the Raman frequencies and intensities.

III. RESULTS

Raman spectra of $Ba_2Cu_xZn_{1-x}WO_6$ for x between 0.0 and 0.4 and of Ba_2CuWO_6 are shown in Fig. 4. The spectra of the mixed crystals consist of three main lines, at 120, 430 and 820 cm^{-1} which positions do not change significantly with x ($0.0 < x < 0.4$). Two additional weak transitions are indicated in the high resolution spectrum of the Ba_2ZnWO_6 host solid at 530 and 750 cm^{-1} (Fig. 5) and found to persist in the spectra of the Cu^{2+} doped samples. As the Cu^{2+} concentration increases the intensity of the 750 cm^{-1} transition grows and a further transition appears at 55 cm^{-1}. Passing to the Ba_2CuWO_6 we note a drastic change in the Raman spectrum, both with respect to the intensities and the positions of the Raman bands (Fig. 6). The 820 cm^{-1} line slightly shifts to lower energies and seems to integrate the former 750 cm^{-1} transition, giving rise to a rather broad band, while an additional weaker component is detected at 664 cm^{-1}. The Raman lines for the mixed crystals at 120 and 430 cm^{-1} are significantly shifted and split by about 65 cm^{-1}, yielding two pairs of transitions at 152, 220 cm^{-1} and 308, 370 cm^{-1}. In order to interpret the experimental results a factor group analysis of the lattice vibrations has been performed for the Ba_2ZnWO_6 (*Fm*3*m*

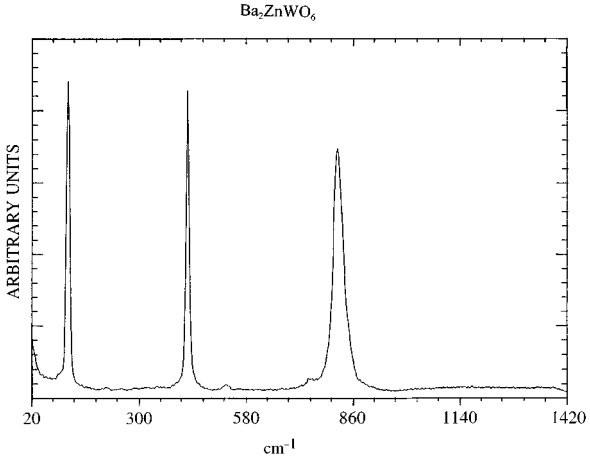

FIG. 5. The Raman spectrum of Ba_2ZnWO_6 (at 300 K).

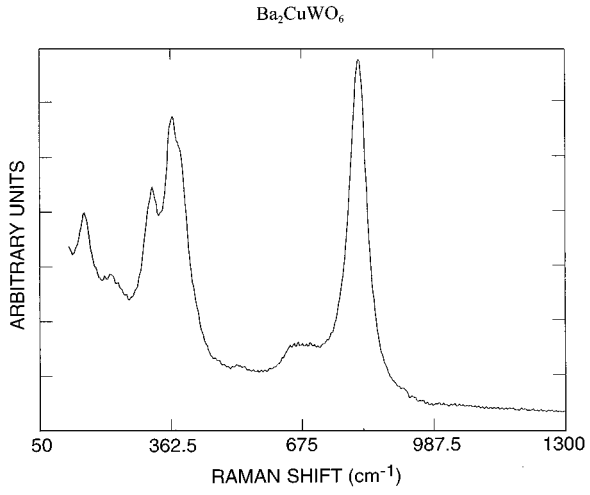

FIG. 6. The Raman spectrum of Ba_2CuWO_6 (at 300 K).

space group). The atomic displacements for the Zn(W), Ba, and O ions occupying sites of O_h, T_d, and C_{4v} point symmetries, respectively, are integrated into (O_h) factor group species, to give four Raman active modes with A_{1g}, E_g, and T_{2g} ($2\times$) symmetry (Table 1). Theoretical calculations on $W(OH)_6$ model clusters (see below) allow to assign these

TABLE 1
Factor Group Analysis for Ba_2ZnWO_6

Ions	Site symmetry (species)	O_h factor group symmetry (species)
Zn(W)	O_h	O_h
	T_{1u}	T_{1u}
Ba	T_d	O_h
	T_2	T_{2g}
		T_{1u}
O	C_{4v}	O_h
	A_1	A_{1g}
		E_g
		T_{1u}
	E	T_{1g}
		T_{2g}
		T_{2u}

Note. Space group symmetry: *Fm3m*. Number of molecules in the unit cell $Z = 4$. Number of molecules in the Bravais space = 1.

$$\Gamma_{\text{crystal vibrations}} = \Gamma_{Ba} + \Gamma_{Zn} + \Gamma_{W} + \Gamma_{O} - \Gamma_{\text{accoust}}$$
$$= 4T_{1u}(\text{IR}) + 2T_{2g}(\text{R}) + A_{1g}(\text{R}) + E_g(\text{R}) + T_{1g} + T_{2u}.$$

modes to the Raman lines at 820, 750, 430, and 120 cm^{-1}, respectively. The two lines at higher energies (750 and 820 cm^{-1}) are predominantly attributed to vibrations of the WO_6 cluster. Symmetry lowering from the O_h (Ba_2ZnWO_6, space group *Fm3m*) to the D_{4h} factor group (Ba_2CuWO_6, space group I4/*mmm*) leads to splittings (E_g into B_{1g}, A_{1g}, and T_{2g} into B_{2g}, E_g) and energy shifts with the tentative assignment of the Raman lines at 152, 220, 308, 370, 664 cm^{-1} to $E_g, B_{2g}, B_{2g}, E_g, B_{1g}$ fundamentals, respectively, and of the broad band at 806 cm^{-1} to the A_{1g} modes (From E_g and A_{1g} in O_h). The origin of the bands at 55 and 530 cm^{-1} is not fully understood. These bands are possibly due to correlated vibrations of the CuO_6 and WO_6 moieties, involving predominantly the CuO_6- and the WO_6-polyhedra, respectively.

IV. DISCUSSION

The intensity increase of the 750 cm^{-1} Raman transition with increasing x can be led back to the Jahn–Teller properties of the Cu^{2+} cations and hence their tendency to distort the next-nearest surrounding. As far as these geometrical changes take place within the cubic symmetry (see the phase line in Fig. 2c, $0.0 < x < 0.2$, 300 K) a distorted surrounding according to elongated octahedra around Cu^{2+} will necessarily impose local distortions on the WO_6 polyhedra in the opposite direction. In order to analyze the effect of such distortions on the Raman energies and intensities we performed calculations of the Raman frequencies and polarization tensors for an octahedral $W(OH)_6$ model cluster adopting W–O (1.868 Å) and O–H (0.951 Å) bond distances, optimized using a SBK basis, in comparison with analogous results for a tetragonally compressed $W(OH)_6$ octahedron [W–O bond lengths: axial 1.828 Å ($2\times$) and equatorial 1.888 Å ($4\times$)]. The OH group has been approximated as a rigid moiety. A set of calculations in which the O–H group was considered as nonrigid did not change the results. The Raman active modes A_{1g}, E_g, and T_{2g} of an *isolated* octahedral MO_6 cluster are depicted in Fig. 3. Raman frequencies, polarizability tensor components α_{kl} and relative intensities of the Raman lines, deduced from the relation in Eq. [2], are listed in Table 2. The results indicate that, for an undistorted $W(OH)_6$ octahedron, A_{1g} should be the most intense transition and E_g of the weakest intensity. Symmetry lowering to D_{4h} induces striking intensity changes only for the $A_{1g}(2)$ component of the parent octahedral E_g vibration, gaining intensity via mixing with the $A_{1g}(1)$ breathing vibration. The extent of intermixing depends on the magnitude of polyhedron distortion which becomes larger as the Cu^{2+} concentration increases. Therefore E_g vibrations mainly confined to WO_6 clusters reflect in an indirect way structural changes due to the replacement of Zn^{2+} by Cu^{2+} in neighboring ZnO_6 polyhedra. The strain imposed by Jahn–Teller distorted CuO_6 centers on

TABLE 2
Calculated Raman Frequencies, Polarizability Tensor Components, and Intensities for *Isolated* Octahedral (O_h) and Distorted Octahedral D_{4h} (Tetragonally Compressed) $W(OH)_6$ Model Clusters

Raman active normal modes Q (O_h symm.)	Raman energies (cm^{-1})	Polariz. tensor components α_{ij} (a.u.)	Raman intensities (a.u./Å^2)	Raman active normal modes Q (D_{4h} symm.)	Raman energies (cm^{-1})	Polariz. tensor components α_{ij} (a.u.)	Raman intensities (a.u./Å)
A_{1g}	856	$\alpha_{xx,yy,zz}$ $(59 - 25Q\alpha_{1g})$	625	A_{1g} (1)	877	$\alpha_{xx,yy}$ $(59 + 24Q\alpha_{1g})$	576
						α_{zz} $(58 + 25Q\alpha_{1g})$	625
E_g	670	α_{xx} $(59 + 4Q\varepsilon_g)$	16	A_{1g} (2)	695	$\alpha_{xx,yy}$ $(59 - 11Q\alpha_{1g})$	121
		α_{yy} $(59 - 4Q\varepsilon_g)$	16				
						α_{zz} $(58 - 0.1Q\alpha_{1g})$	0
				B_{1g}	631	α_{xx} $(59 + 2.5Q\beta_{1g})$	6
						α_{yy} $(59 - 3.5Q\beta_{1g})$	12
T_{2g}	794	$\alpha_{xy,xz,yz}$ $(15Q\tau_{2g})$	225	B_{2g}	794	α_{xy} $(15Q\beta_{2g})$	225
				E_g	794	$\alpha_{xz,yz}$ $(15Q\varepsilon_g)$	225

Note. Adopted W–O and O–H bond lengths for the octahedral $W(OH)_6$ cluster are those obtained by a geometry optimization using effective core potentials (SBK basis); R(W–O) = 1.868 Å and R(O–H) = 0.951 Å. Data for D_{4h} refer to a tetragonally compressed octahedron with $R(W–O)_{ax} = R(W–O) - 0.04$ Å, $R(W–O)_{eq} = R(W–O) + 0.02$ Å and with an unaltered O–H distance.

neighboring WO_6 polyhedra in the cubic phase ($x \leq 0.2$) becomes larger in the tetragonal phase ($x = 0.3, 0.4$) leading to a remarkable intensity increase of the $A_{1g}(2)$ mode in the latter case. The calculated Raman energies for the A_{1g} and E_g modes of the $W(OH)_6$ octahedron roughly match with those observed at 820 and 750 cm^{-1}, indicating that these vibrations are nearly completely confined to the WO_6 entitites in the $Ba_2Cu_xZn_{1-x}WO_6$ mixed crystals. The T_{2g} mode at 430 cm^{-1} seems to be strongly coupled with vibrational motions of the neighbored $Zn(Cu)O_6$ polyhedra, however—hence appearing at considerably lower energy than calculated (794 cm^{-1}; Table 2).

The Raman spectra of the mixed crystals ($x \leq 0.4$) reflect a redistribution of Raman intensity from the $A_{1g}(1)$ to the $A_{1g}(2)$ mode of E_g due to the symmetry lowering from O_h to D_{4h}, without altering the band maxima positions significantly. In contrast, the spectrum of Ba_2CuWO_6 displays a strongly changed Raman pattern involving both energy shifts and line splittings. These reflect the increase of the local distortion of the WO_6 octahedra when moving from Ba_2ZnWO_6 to Ba_2CuWO_6, caused by specific changes of the elastic properties of the bridging oxygen ions by the long-range cooperative ordering pattern (2). The enhanced splitting of the E_g vibration leads to a near-coincidence of the $A_{1g}(2)$ split mode with $A_{1g}(1)$. The assignment of the Raman pairs to the tetragonally splitted T_{2g} vibrational states at 152 cm^{-1} (E_g), 220 cm^{-1} (B_{2g}), and 308 (B_{2g}), 370 cm^{-1} (E_g), which we attribute to elastically coupled symmetrized displacements from predominantly CuO_6 octahedra (elongation) and from mainly WO_6 octahedra (compression), respectively, reflect the different sign of the octahedral distortions around Cu and W. It should be reminded here that the tetragonal B_{2g} component of the parent octahedral vibrational state T_{2g} involves equatorial ligands only, while the E_g components include angular distortions with participation from both equatorial and axial M–O bonds (see Fig. 3). The intensity relations (see Fig. 6) support the assignment, because an E_g transition is expected to have (by statistical reasoning) about twice the intensity of B_{2g}. It is also in agreement with the proposed assignment, that the centre of gravity of the two T_{2g} states is nearly identical for the mixed crystals ($x \leq 0.4$), namely 275 cm^{-1}, and for Ba_2CuWO_6 (262 cm^{-1}), though the energies of the T_{2g} split modes lie much closer in the latter case.

IV. CONCLUSION

1. The Raman spectra of $Ba_2Cu_xZn_{1-x}WO_6$ mixed crystals are found to reflect an interesting dependence of the

intensity of the Jahn–Teller active octahedral E_g mode on the Cu^{2+} concentration. The gain of intensity for the $A_{1g}(E_g)$ split component—involving predominantly compressed WO_6 octahedra ($750\,cm^{-1}$)—can be used as a rather sensitive probe for detecting structural changes due to the vibronically active Cu^{2+} ion, which induces environmental distortions of neighbouring non-Jahn–Teller ions (W^{6+}) as well.

2. A consistent assignment of the Raman lines observed at 150 and $430\,cm^{-1}$ ($x \leq 0.4$) is possible on the basis of coupled bending motions of the WO_6 and $Zn(Cu)O_6$ octahedra with T_{2g} symmetry. The transition from local distortions in the octahedral framework of the cubic elpasolite lattice due to the incorporation of Cu^{2+} to the long-range cooperative Jahn–Teller order in tetragonal Ba_2CuWO_6 is accompanied by drastic changes in the spectral appearance (Figs. 4–6).

ACKNOWLEDGMENTS

This study was supported financially by a NATO research grant. Thanks are due to Prof. Dr. G. H. Wolf, Arizona State University, for supplying the Raman spectra.

REFERENCES

1. D. Reinen and C. Friebel, *Struct. Bonding* **37,** 1 (1979).
2. D. Reinen and M. Atanasov, *Magn. Res. Rev.* **15,** 167 (1991).
3. D. Reinen and H. Weitzel, *Z. Anorg. Allg. Chem.* **424,** 31 (1976).
4. D. J. Durben and G. H. Wolf, *Phys. Rev. B* **43,** 2355 (1991).
5. M. W. Schmidt, K. K. Baldridge, J. A. Boatz, S. T. Elbert, M. S. Gordon, J. H. Jensen, S. Koseki, M. Matsunaga, K. Nguyen, S. J. Su, T. L. Windus, M. Dupuis, and J. A. Montgomery, *J. Comput. Chem.* **14,** 1347 (1993).
6. (a) W. J. Stevens, H. Basch, and M. Krauss, *J. Chem. Phys.* **81,** 6026 (1984); (b) W. J. Stevens, H. Basch, M. Krauss, and P. Jasien, *Can. J. Chem.* **70,** 612 (1992); (c) T. R. Cundary and W. J. Stevens, *J. Chem. Phys.* **98,** 5555 (1993).